Protein Science (1996), *5*:1366–1375. Cambridge University Press. Printed in the USA.

Novel isolation method and structural stability of a eukaryotic chaperonin: The TCP-1 ring complex from rabbit reticulocytes

MONA TREMPE NORCUM

Department of Biochemistry, University of Mississippi Medical Center, Jackson, Mississippi 39216-4505

(RECEIVED December 27, 1995; ACCEPTED April 22, 1996)

Abstract

In the course of removing a contaminant from preparations of aminoacyl-tRNA synthetase complexes, a novel purification method has been developed for the eukaryotic cytoplasmic chaperonin known as TRiC or CCT. This method uses only three steps: ammonium sulfate precipitation, pelleting into a sucrose cushion, and heparin-agarose chromatography. As judged by electrophoresis, sedimentation, and electron microscopy, the preparations are homogeneous. The particle is identified as a chaperonin from electrophoretic polypeptide pattern, electron microscopic images, direct mass measurement by sedimentation velocity analysis, amino-terminal sequencing, and ATP-dependent refolding of rhodanese and actin.

Further investigation of the biochemical and physical properties of the particle demonstrates that its constituent polypeptides are not glycosylated. The particle as a whole binds strongly to polyanionic matrices. Of particular note is that negatively stained images of chaperonin adsorbed to a single carbon layer are distinctly different from those where it is sandwiched between two layers. In the former, the "characteristic" ring and four-stripe barrel predominate. In the latter, most images are round with a highly reticulated surface, the average particle diameter increases from 15 to 18 nm, and additional side, end, and substrate-containing views are observed. The particle structure is strikingly resistant to physical forces (long-term storage, repeated cycles of freezing and thawing, sedimentation), detergents (Triton, deoxycholate), salts (molar levels of KCl or LiCl), and pH changes (9–6). Only a strongly chaotropic salt (NaSCN) and extremely acidic conditions (pH 4.5) cause aggregation and dissociation of TRiC, respectively. However, treatment with KCl or deoxycholate reduces TRiC folding activity.

Keywords: electron microscopy; eukaryotic chaperonin; mass measurement; protein folding; protein purification; protein structure

Over the last two years, routine preparations of the multienzyme complex of aminoacyl-tRNA synthetases from rabbit reticulocyte lysate (Norcum, 1991) had become increasingly contaminated. In the course of determining the cause of the contamination, and in eliminating the problem, the contaminant has been identified as a eukaryotic chaperonin particle, specifically the TCP-1 ring complex.

Molecular chaperones are proteins and protein complexes that aid the process of folding and assembly of polypeptide structures (Ellis, 1993). Chaperonins constitute a particular class of chaperones that are characterized by their ubiquity, double-ringed cylindrical structure, ATPase activity, and ability to bind a variety of unfolded protein substrates (Horwich & Willison, 1993; Gupta, 1995). There are two distinct families or groups of chaperonins. One is composed of the eubacterial and organellar homooligomers typified by GroEL and Hsp60. The heterooligomeric chaperonins from archaebacteria and eukaryotes constitute the second class. These include TF55, the thermosome, and the cytosolic chaperonin from eukaryotes, which is known as TRiC or CCT. The known properties of the eukaryotic chaperonin have been reviewed thoroughly in a recent paper (Kubota et al., 1995).

Most of the recent literature on TRiC is concerned with its role in assisting folding of proteins. Substrates described to date range from tubulin and actins (Yaffe et al., 1992; Melki & Cowan, 1994) to nascent luciferase (Frydman et al., 1994) and a viral capsid assembly (Lingappa et al., 1994). Much progress has also been made toward identifying the numbers and types of

Reprint requests to: Mona Trempe Norcum, Biochemistry Department, University of Mississippi Medical Center, 2500 North State Street, Jackson, Mississippi 39216-4505; e-mail: mnorcum@fiona.umsmed.edu.

Abbreviations: ANS, anilinonaphthalene sulfonic acid; DOC, deoxycholate; TCP-1, t-complex polypeptide; TRiC, TCP-1 ring complex; PMSF, phenylmethylsulfonyl fluoride; TAME, *Nα-p*-tosyl-L-arginine methyl ester.

subunits in the eukaryotic chaperonin, most notably the cloning of eight TCP-1 related genes in the mouse (Kubota et al., 1995, and references therein). Although averaged images of the particle with and without bound substrate have been presented (Marco et al., 1994), detailed information about the structural and biochemical properties of the eukaryotic chaperonin particle is still sparse. This may be due in part to the limitations of isolation procedures that rely on size fractionation, limited capacity affinity supports, and laborious folding assays (Frydman et al., 1992; Gao et al., 1992; Lewis et al., 1992).

This study describes a novel isolation protocol for TRiC that yields milligram quantities of electron microscopically homogeneous material using only three steps, all of which are common and inexpensive biochemical methods. Several physical and biochemical properties of the particle are presented, including direct mass analysis from sedimentation velocity data. In addition, new types of images have been observed in negatively stained electron micrographs. The structural stability of the particle has been assessed by determining the effect of detergents, salts, or pH on its electron microscopic appearance. Finally, a fluorescence-based assay has been adapted for quantitative comparison of the ATP-dependent refolding activities of TRiC.

Results

Isolation

The chaperonin particle (TRiC) from rabbit reticulocyte lysate was purified using only three steps: ammonium sulfate precipitation, centrifugation into a sucrose cushion, and chromatography on heparin-Sepharose. All of these are common biochemical techniques using reagents and materials that are available readily from commercial sources. Details of the procedure are given in the Materials and methods. The material prepared by this method is extremely homogeneous, as demonstrated by SDS-PAGE (Fig. 1), electron microscopy (Fig. 2), and sedimentation velocity analysis (Fig. 3). Large amounts of starting material can be processed easily by this protocol, and yields of purified particle are high. Typically greater than 6 mg is obtained per isolation from reticulocytes. This is equivalent to 0.03–0.05% of lysate protein, or 0.1–0.25 mg/mL packed cells.

Biochemical and physical properties

One-dimensional SDS-PAGE (Fig. 1) indicates that the chaperonin particle as prepared above is composed of at least four polypeptides, with apparent masses of 70, 66, 62, and 60 kDa. Densitometric scanning gives ratios of 1:2:2:1, respectively, relative to the 70-kDa band. The 66- and 62-kDa bands can be resolved into closely spaced doublets when much less protein is electrophoresed (data not shown).

In negatively stained electron micrographs, the particle is seen to be extremely regular in size and shape. In areas of a single-carbon layer (Fig. 2A), the predominant view is of a ring with a central stain-filled hole. Barrel-shaped double-ring structures are also observed. In areas of double-carbon layers (Fig. 2B), almost all images are of a cage-like structure resembling an icosahedron. The average particle diameter is 15–18 nm, with the smaller measurement derived from single-carbon images and the larger from double-carbon images.

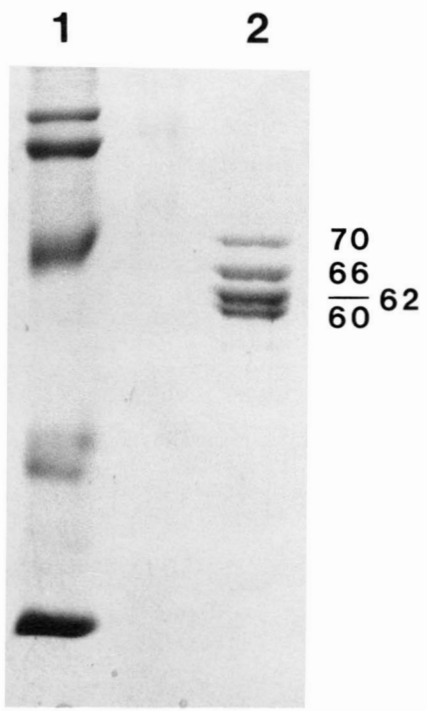

Fig. 1. Polypeptide pattern of rabbit reticulocyte chaperonin upon SDS-PAGE using a 10% gel. Lane 1, Molecular mass standards (116, 97.4, 66, 45, and 29 kDa); lane 2, 0.75 μg of protein. Apparent polypeptide mass in kDa.

Sedimentation velocity analysis (Fig. 3) indicates that the particle is also homogeneous in mass. The distribution of sedimentation coefficients shows a single major peak at 27.2 *S*. When corrected for temperature and buffer components, the $S_{20,w}$ is 24.8, from which the particle mass is calculated to be 775–950 kDa. Taken together with the electrophoretic pattern and stoichiometry, this suggests that the particle contains 12–14 polypeptides.

From attempts to perform gas phase amino-terminal microsequencing of the polypeptides, it is clear that all but the 60-kDa polypeptide are N-terminal blocked. The blocking groups are resistant to both HCl and trifluoroacetic acid treatment. Partial sequence information was obtained using the 60-kDa band as well as the whole protein mixture. Both yielded the same amino-terminal sequence (Fig. 4).

There is no reaction of the particle polypeptides either in polyacrylamide gels (Copeland, 1994) or on nitrocellulose membranes (Thornton et al., 1994) with classic carbohydrate staining reagents, including periodic acid-Schiff reagent, thymol-sulfuric acid, and alcian blue (data not shown). Thus, none appear to be glycosylated. Rather striking is the affinity of the particle for the polyanionic chromatographic matrix, heparin-Sepharose. It also binds strongly to tRNA immobilized on agarose (data not shown). This is not simply an ability to bind to negatively charged supports, because none of the particle is retained on the strong cation exchange resin S-Sepharose at comparable pH and ionic conditions.

The purified material has ATPase activity, the average being 4.8 ± 1.0 nmol of phosphate released per milligram of protein per minute at 37 °C.

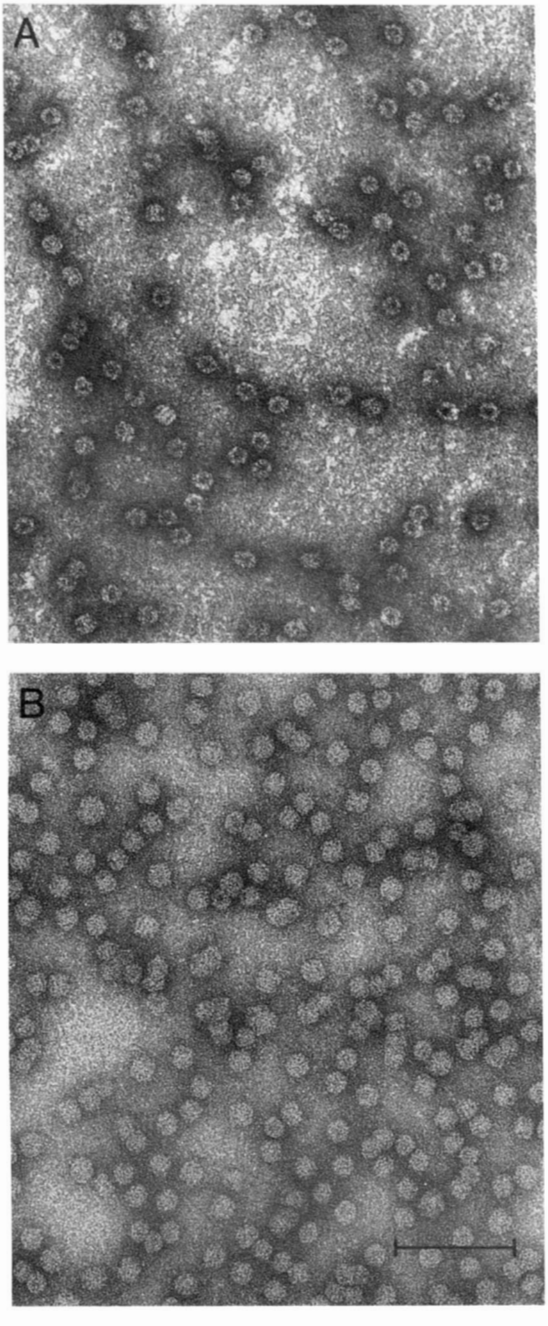

Fig. 2. Electron micrographs of negatively stained rabbit reticulocyte chaperonin. Size bar = 100 nm. **A:** Area of single carbon layer staining. **B:** Area of double carbon layers.

Analysis of electron microscopic images

As presented in Figure 5, several types of images are observed commonly in negatively stained electron micrographs of these preparations. The star-like ring and four-stripe barrel views that are characteristic of chaperonins (rows 1 and 2) have been described previously by a variety of investigators. These two images predominate in single-carbon layer areas (Fig. 2A), but in double-carbon layer areas (Fig. 2B), most particles have a more uniform round appearance.

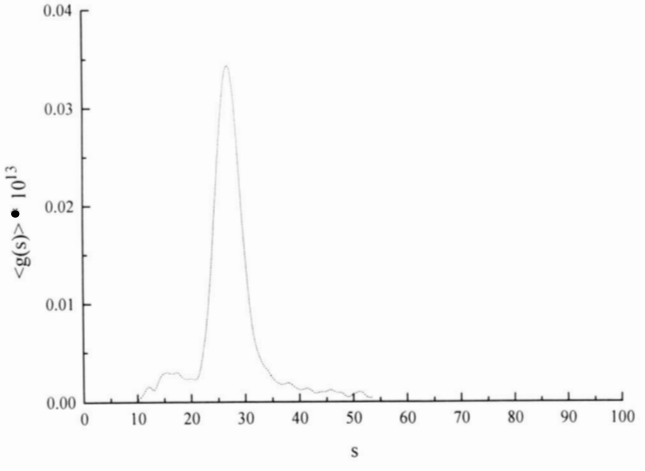

Fig. 3. Distribution of apparent sedimentation coefficients of rabbit reticulocyte chaperonin.

When the latter images are enlarged, the particle surface appears highly reticulated (row 3), with numerous small areas of stain penetration. These appear to be variations of the typical four-stripe orientation that are due to tilting of the particle or the effect of sandwiching it between two carbon layers. The latter leads to a thinner and more uniform distribution of stain, but may also flatten the structures somewhat. However, such images correlate intriguingly with the existence of "windows" distributed around each of the rings of the GroEL chaperonin crystal structure (Braig et al., 1994). Another class of double-carbon layer images are octagonal, reflecting the eightfold symmetry of this class of chaperonins (Kubota et al., 1995). These views also have only small areas of interior stain penetration (row 4). This suggests that they could be end views of "closed" barrels, analogous to that of the GroEL–GroES complex (Langer et al., 1992; Chen et al., 1994), or as predicted from a three-dimensional reconstruction of the thermosome (Phipps et al., 1993), which shows caps for each ring.

Occasional variations in the characteristic images are also seen. In row 5 are examples of the four-stripe barrels with either protein protruding from or a clear opening in one end. Row 6 contains ring views in which stain is partially excluded from the central channel. All of these images are consistent with chaperonin molecules that either are complexed with substrate or are prepared to do so. For both prokaryotic (Braig et al., 1993) and eukaryotic (Chen et al., 1994; Marco et al., 1994) chaperonins, folding substrates bind at the central channel of the particle. In addition, the functional prokaryotic holo-chaperonin is distinctly asymmetric (Langer et al., 1992) with one end closed and the distal ring appearing fragmented or "open."

```
60 kDa band:     P-E-N-V-A-P-R-S-G-G-P-A-G-A-A-G-G-R-D
                 | | | | |   | | |   |
Mouse CCT-δ:  M-P-E-N-V-A-S-R-S-G-A-P-T-A-G-P-S-R-G-K
```

Fig. 4. Comparison of the amino-terminal sequence of rabbit chaperonin 60-kDa polypeptide obtained by direct gas-phase sequencing with that deduced for mouse CCT-δ from the nucleotide sequence of its cDNA clone (Kubota et al., 1994).

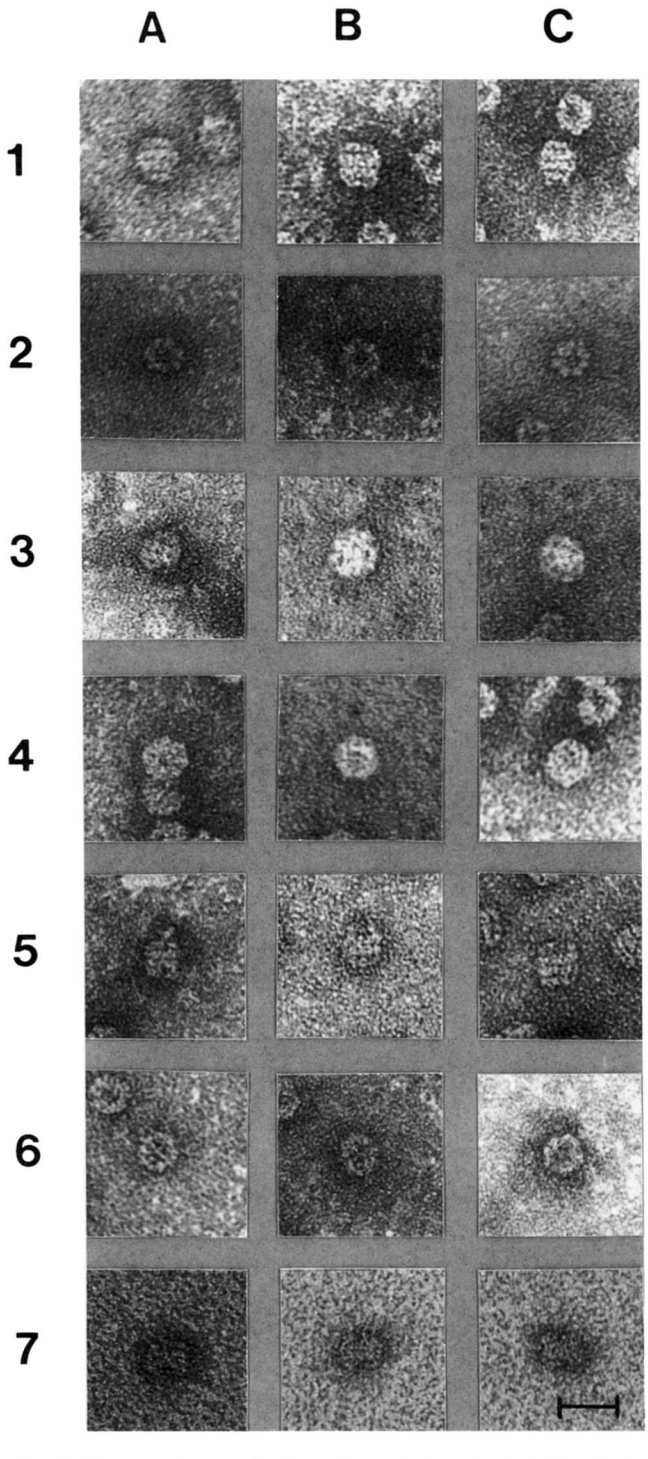

Fig. 5. Electron microscopic views of negatively stained rabbit reticulocyte chaperonin. Size bar = 25 nm. Row 1, side view four-stripe barrels; row 2, single-carbon end view rings with empty central channel; row 3, double-carbon cages; row 4, octagons; row 5, barrels with protruding protein or "open" ring ends; row 6, end views with filled central channel; row 7, novel edge view.

A novel rectangular class of images is presented in row 7. Indentations occur at the center of each edge along the long axis and longitudinal striations are visible in some images (7A). These are seen most often in fractions of density gradient purified TRiC, so represent particles that are of comparable mass as the other types of images. Moreover, all observed to date are in areas of double-carbon layers. Possible interpretations are that these images result when most or all of the outer rings of the barrel are obscured due to a tilted orientation of the particle on the support film. This would be accentuated by "wrapping" of carbon layers around the particle (Kellenberger et al., 1982), that is, the support film is flexible and particulate samples can actually sink into it.

Structural stability

Having been initially intrigued by the remarkable uniformity of TRiC preparations even after storage at −20 °C for more than two years, additional studies on the structural stability of the particle were conducted. As demonstrated in Figure 6, the particle is essentially unaffected by a variety of treatments that are often extremely disruptive of protein–protein interactions.

Specifically, negatively stained electron micrographs of TRiC after repeated cycles of freezing and thawing (Fig. 6A) maintain almost the same uniformity of particle size and shape as for material that has been prevented from freezing by storage in high glycerol buffer (compare with Fig. 2). All characteristic views are visible with only an occasional misshapen particle. The sole effect of the nonionic detergent Triton X-114 is to emphasize the characteristic double-ring or four-stripe chaperonin images in electron micrographs (Fig. 6B). Similar to the physical stresses of freezing and thawing, the anionic detergent deoxycholate has no significant effect on the appearance of the particle (Fig. 6C). Even in the presence of molar concentrations of KCl (Fig. 6D) or the chaotropic salt LiCl (Fig. 6E), less than 5% of the images indicate an effect on the overall structure. The altered images appear as opened rings or collapsed particles. However, incubation with NaSCN eliminates all characteristic images and induces formation of large aggregates.

The structure is also stable over a wide range of pH (Fig. 7). After incubation in buffers from pH 9 (Fig. 7A) to pH 6 (Fig. 7B), the uniformity of size and shape is apparent and all of the characteristic views are present. About 50% of the assembled particle even persists for a short time at pH 4.5 (Fig. 7C), but after a longer incubation time (Fig. 7D, inset), only individual polypeptides and a few very small complexes are seen.

Thus, the assembled TRiC particle is astoundingly stable—only a strongly denaturing detergent (SDS), the most chaotropic anion (isothiocyanate), or an extreme of pH (4.5) are able to dissociate the chaperonin complex.

Chaperonin activity

Anilinonaphthalene sulfonate compounds become highly fluorescent in apolar environments and so are extremely sensitive probes for hydrophobic regions of proteins. Change in fluorescence of 1,8-ANS has been used to quantitate folding of rhodanese and dihydrofolate reductase by the prokaryotic chaperonin GroEL (Martin et al., 1991). A similar assay has been used in this study to demonstrate the folding activity of eukaryotic chaperonin isolated by this new procedure and to assess the effects of salt and detergent treatment on this activity.

As seen in Figure 8A, the fluorescence emission spectra of 2,6-ANS in the presence of either native or denatured rhodanese are identical, with a maximum at 460 nm. These curves are also

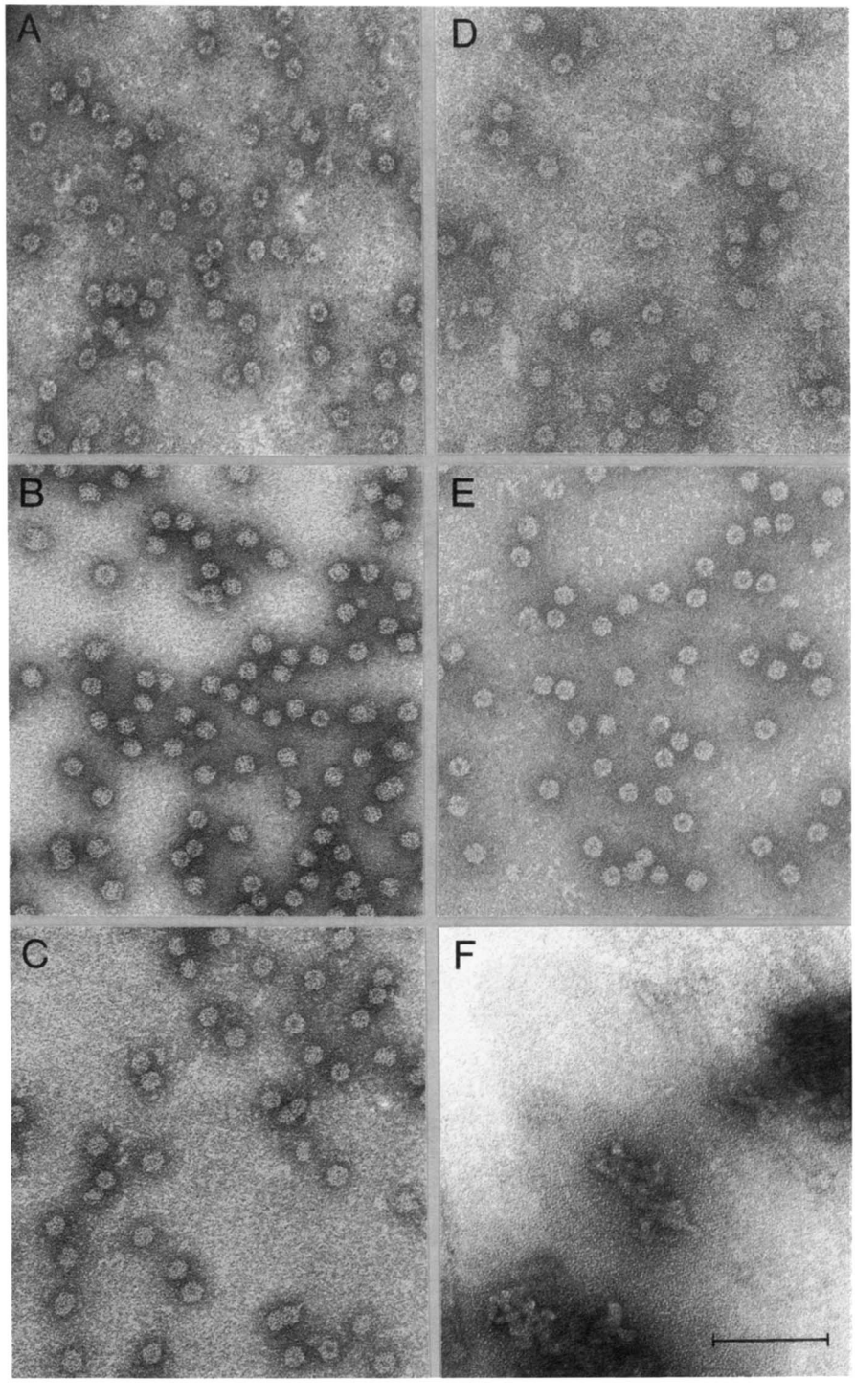

Fig. 6. Electron micrographs of negatively stained rabbit reticulocyte chaperonin after a variety of treatments to test structural stability. Size bar = 100 nm. **A:** Repeated freeze/thaw. **B:** Extracted with 1% Triton X-114. **C:** Incubated with 1.6 mM DOC. **D:** Incubated with 1.1 M KCl. **E:** Incubated with 0.9 M LiCl. **F:** Incubated with 0.9 M NaSCN.

identical to that observed for ANS in buffer only (data not shown). In the presence of TRiC, there is the typical marked enhancement of fluorescence intensity and shift of the emission maximum toward 440 nm (Mock et al., 1988). Addition of native rhodanese to the chaperonin does not alter the spectrum. However, a significant increase in ANS fluorescence is seen when denatured rhodanese is added. This has been attributed to binding of ANS to hydrophobic regions of early folding intermediates bound to chaperonin complexes (Martin et al., 1991). Figure 8B shows a similar effect using actin as a folding substrate. That is, additional ANS fluorescence over the background of TRiC alone is induced by denatured actin, but not native actin. Again, there is no difference in ANS binding between the native and denatured substrate, so the increase is due to the action of the chaperonin.

In both cases, the folding process is completed upon addition of MgATP. This is indicated by the return of ANS fluorescence to the level of native substrate (Fig. 9A). That is, in the pres-

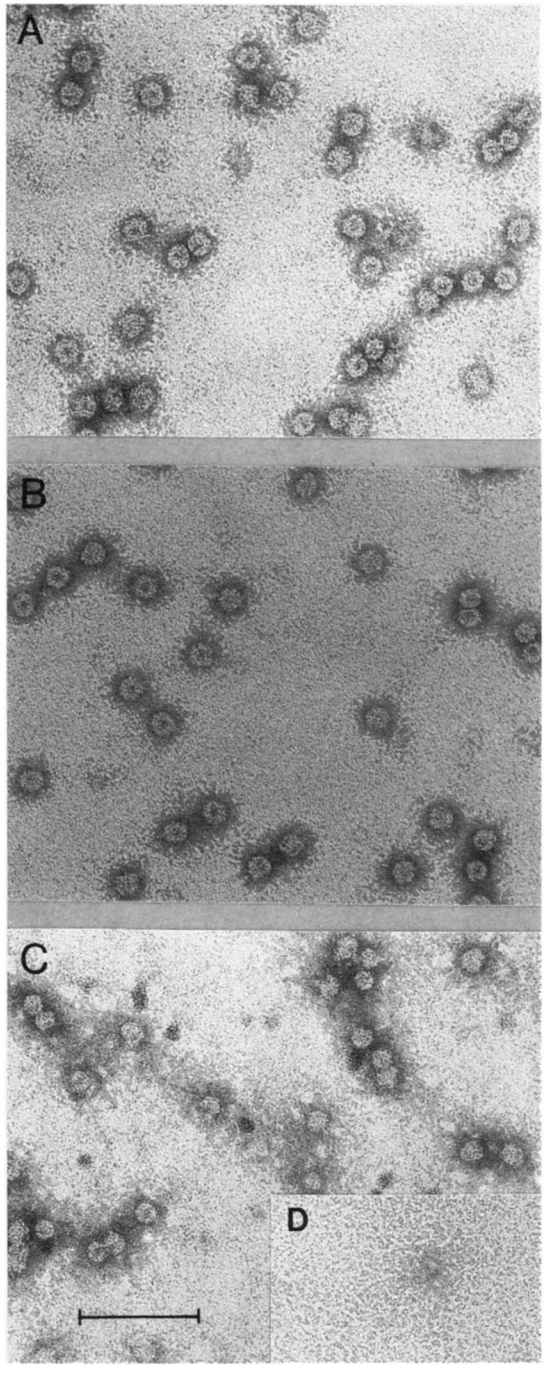

Fig. 7. Electron micrographs of negatively stained rabbit reticulocyte chaperonin demonstrating the effect of pH on the particle. Size bar = 100 nm. **A:** 50 mM sodium borate, pH 9. **B:** 50 mM sodium acetate, pH 6. **C:** 50 mM ammonium acetate, pH 4.5. **D:** Inset, additional time at pH 4.5.

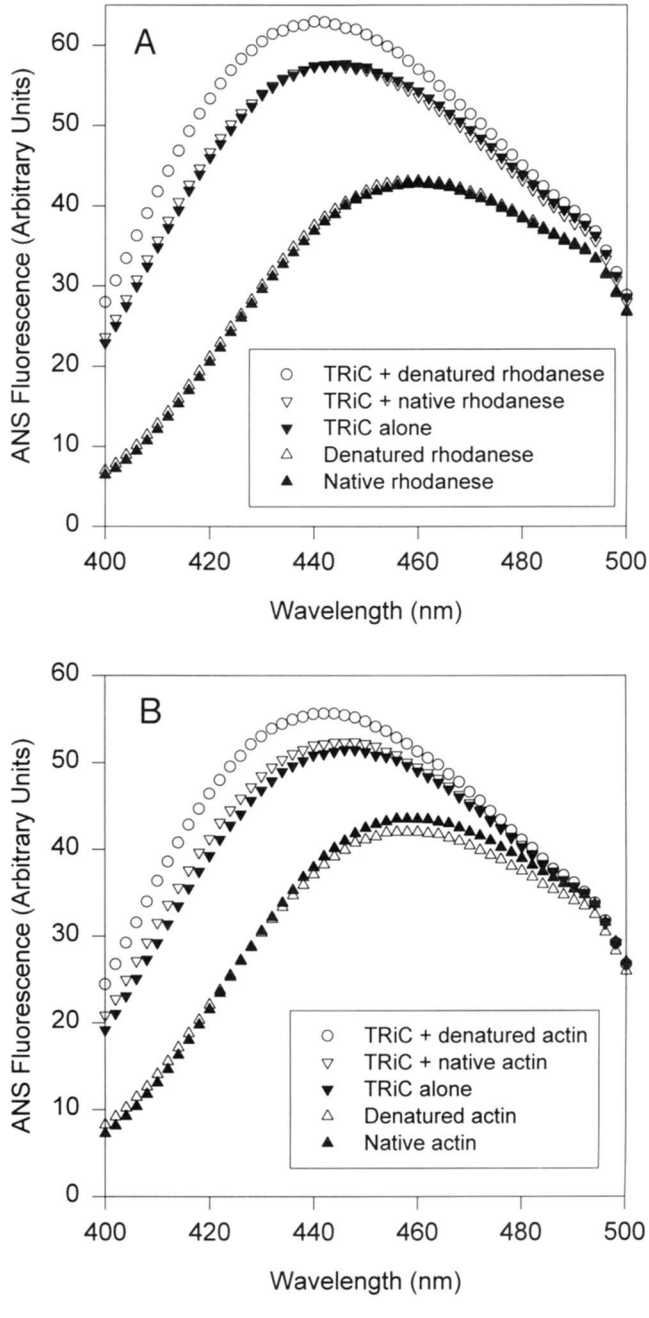

Fig. 8. ANS fluorescence in the presence of TRiC, native, or denatured substrate proteins. Samples contained TRiC, native, and denatured rhodanese (**A**) or actin (**B**) each separately and as chaperonin/substrate combinations. Curves shown are the average of four emission spectra with excitation at 325 nm. For clarity, only every other data point is plotted.

ence of denatured rhodanese, there is an average fourfold enhancement of signal over native protein. This is effectively eliminated upon refolding. Denatured actin induces a comparable increase in ANS fluorescence, which is also reduced markedly in an ATP-dependent manner. Although within a standard deviation of the value for native protein, the higher residual signal may indicate that the refolding of actin is less efficient under these conditions. The net ANS fluorescence seen with native substrates is the same before or after incubation with ATP (data not shown).

Although no major structural changes were seen after treatment of TRiC with most of the salts and detergents tried, these reagents might induce subtle changes that could affect folding ability. To test this possibility, rhodanese was chosen as a substrate because the change in ANS fluorescence upon its refold-

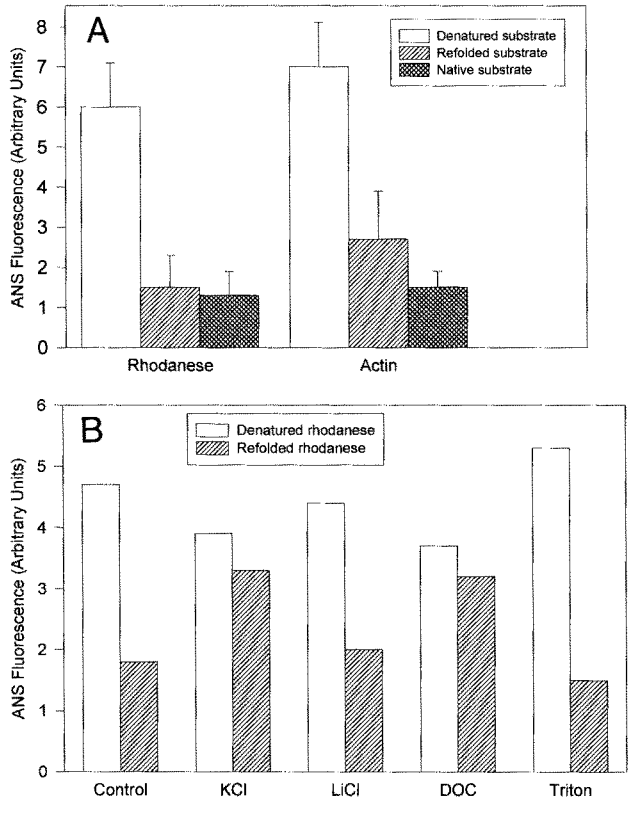

Fig. 9. ATP-dependent refolding of denatured substrates by TRiC as monitored by change in ANS fluorescence. Emission was measured at 430 nm, with excitation at 325 nm. Spectra for refolded substrates were of aliquots of the same mixtures containing denatured substrates, but after 40 min at 30 °C in the presence of MgATP. **A:** Comparison of refolding of rhodanese and actin by TRiC. Values are the average for three different preparations. **B:** Effect of salts and detergents on the refolding of rhodanese by TRiC. Chaperonin was incubated with 1.1 M KCl, 0.9 M LiCl, 1.6 mM DOC, or 1% Triton X-114, then exchanged into assay buffer by gel filtration. A representative experiment is shown.

ing has been characterized previously (Martin et al., 1991) and it was the most efficiently folded of the substrates tried. In the experiment shown (Fig. 9B), the usual increase in ANS fluorescence was observed upon addition of denatured rhodanese in all cases, and the magnitude of the increase was comparable to control chaperonin. Thus, prior incubation with KCl, LiCl, DOC, and Triton do not affect the initial ATP-independent interaction between TRiC and unfolded protein. Neither LiCl nor Triton affected the ATP-dependent decrease in ANS fluorescence significantly. However, both KCl and DOC inhibited completion of rhodanese refolding. The effect of basic or acidic pH conditions on the ability of TRiC to fold proteins was not tested because no ATPase activity was measurable over the increased background at pH 8.5 and 6 (data not shown). It did not appear useful to test the conditions that obviously aggregated or dissociated TRiC.

Discussion

Identification as TRiC

Identification of the particle purified from rabbit reticulocyte lysate as the eukaryotic chaperonin TRiC is based on its composition, size, electron microscopic images, and amino-terminal sequence of the 60-kDa polypeptide.

The one-dimensional SDS-PAGE polypeptide pattern of TRiC from bovine testis (Frydman et al., 1992; Waldmann et al., 1995) and rabbit reticulocytes (Rommelaere et al., 1993) is very similar to that presented here (Fig. 1). The number of bands, stoichiometry, and appearance of closely spaced doublets correlate precisely. The estimated M_r values differ by only 7–10%, which can be accounted for by differences in electrophoretic conditions. The mass of murine, human, and rabbit reticulocyte TRiC has been estimated from density gradient sedimentation (Lewis et al., 1992) and gel filtration (Gao et al., 1992) as 800–950 kDa. Based on measurements of images of unstained protein obtained by scanning transmission electron microscopy, the M_r of bovine TRiC was calculated to be 970 ± 54 kDa (Frydman et al., 1992). These estimated values are comparable to what is derived in this study from direct measurement of the sedimentation coefficient using analytical ultracentrifugation (Fig. 3).

Numerous investigators have published negatively stained images of the TRiC particle. Two types of images are considered characteristic: a four-stripe barrel and a ring with eight-fold rotational symmetry. These side and end views, respectively, have been used to identify chaperonins from a variety of organisms (Saibil & Wood, 1993). As shown in Figure 2 and in rows 1 and 2 of Figure 5, these are present clearly in the material isolated here.

Attempts to sequence the bovine TRiC polypeptides directly indicated that several were blocked at their amino-termini (Frydman et al., 1992). However, polypeptide sequence information has been obtained from cDNA clones of the murine particle (Kubota et al., 1994). The sequence presented here for material isolated from rabbit reticulocytes (Fig. 4) is remarkably similar to that predicted for the δ subunit of the murine particle. That is, 9 of the first 12 amino acids are identical. Overall, the homology score is 56.2% over 16 residues.

Taken together, these data indicate that the particle isolated here is indeed the eukaryotic chaperonin ring complex, TRiC.

Advantages of isolation procedure

The novel purification procedure presented here has several advantages. The method is very simple, rapid, and cost effective, requiring about a day for purification of milligram quantities of homogeneous and highly concentrated material. It uses only common laboratory materials and one relatively inexpensive chromatographic support, which is available in bulk. This allows high throughput of starting material. Also, the usual time-consuming preparative density gradients are eliminated and there is no need for expensive HPLC columns and affinity matrices (Frydman et al., 1992; Gao et al., 1992; Lewis et al., 1992).

Moreover, this method yields extremely homogeneous material consistently, as judged by electrophoresis, sedimentation analysis, and electron microscopy. Throughout the preparation, the polypeptide pattern and ratios are constant, as are the size and images of the purified material. In contrast to other reports, there is no evidence of partial proteolysis (Hynes et al., 1995) or of varying amounts of other proteins, such as hsp 70 (Lewis et al., 1992; Kubota et al., 1994) or folding cofactors (Gao et al., 1993, 1994). The very small amount of low molecular mass material observed in the sedimentation velocity profile is likely as-

sociated substrate, as seen in unusual electron microscopic images (Fig. 5A).

That this procedure yields not just homogeneous but also active chaperonin is demonstrated by its ATPase activity and ability to refold rhodanese and actin. The rate of ATP hydrolysis exhibited by the TRiC purified here is lower than reported previously (Frydman et al., 1992), which may be due to the now complete removal of hsp70, an ATPase that often copurifies with TRiC (Lewis et al., 1992; Gao et al., 1993). However, the rate is higher than that reported for a TRiC analogue, the archaebacterial thermosome (Waldmann et al., 1995). TRiC isolated here efficiently folds both rhodanese and actin in an ATP-dependent manner (Fig. 9). Such folding assays, which use the change in ANS fluorescence as a reflection of the change in formation and accessibility of hydrophobic regions of the substrate proteins, have been used previously to characterize the folding activities of the prokaryotic chaperonin GroEL (Martin et al., 1991). This study extends their application to the eukaryotic particle and to an additional substrate. The advantages of this assay system include simplicity and sensitivity. However, care must be exercised when using substrate proteins denatured with guanidine because residual denaturant alters the background ANS binding of TRiC (data not shown). This effect is seen at as little as 60 mM. This is comparable to the concentration that has been reported to alter markedly the ATPase activity and structure of GroEL/GroES complexes (Todd & Lorimer, 1995).

New properties of TRiC

These studies have extended the list of physical and biochemical characteristics of TRiC. As for bovine chaperonin (Frydman et al., 1992), most of the constituent polypeptides in the rabbit are modified at their amino termini, but there is no evidence of glycosylation. The strong affinity of TRiC for polyanions is intriguing. This might simply be due to the multiple ATP binding sites, which, in the prokaryotic chaperonin, circle the particle exterior (Braig et al., 1994). Alternatively, it is possible that ability to bind to highly charged surfaces may play a role in targeting chaperonins to areas of active protein synthesis, whether through interaction with cytoskeletal proteins (Roobol et al., 1995) or ribonucleoprotein particles and ribosomes (Frydman et al., 1994).

Two aspects of this study are particularly striking. Firstly, there is the distinct difference in appearance of negatively stained TRiC in areas of single-carbon versus double-carbon layers (Figs. 2, 5). Double-carbon layer techniques usually provide increased resolution as a result of the thinness and uniformity of stain (Lake, 1978). However, for hollow structures, such as virus capsids, sandwiching can cause significant flattening of the particle (Kellenberger et al., 1982). The consistently larger diameter measured for TRiC in double-carbon images suggests that some flattening is occurring. This emphasizes the existence of an empty channel through the particle. Very few double-carbon images show the deep stain penetration of the "characteristic" ring and four-stripe barrel. In contrast, the images are predominantly round, with highly reticulated surfaces. Indeed, they closely resemble a space-filling model of the crystal structure of GroEL (Braig et al., 1994). This suggests a stronger influence of drying effects and variation in stain density (Oliver, 1973) on single-carbon images of chaperonins.

Secondly, this study demonstrates the remarkable structural stability of TRiC. Neither physical stresses (repeated freeze/thaw cycles, sedimentation) nor a variety of chemical treatments (high salt, detergents, pH changes) affect the overall structure (Figs. 6, 7). Only the most strongly chaotropic salt (NaSCN) and most acidic pH (4.5) disrupted the complex. The crystal structure of GroEL (Braig et al., 1994) shows a subunit interface of typical van der Waal's contacts with no unusual characteristics other than being about 8% more polar than is typical. By analogy, there is nothing that predicts the imperviousness of TRiC to these dissociative forces.

The robustness of the chaperonin particle extends to some extent to its activity. Neither treatment with LiCl nor the nonionic detergent Triton X-114 affected the ability of TRiC to fold rhodanese (Fig. 9B). It is possible that these reagents do induce changes in the chaperonin, but that these reverse upon exchange into the assay buffer. Indeed, after exposure to molar concentration of another neutral salt, KCl, or to a submicellar concentration of the anionic detergent DOC, the particle is no longer able to refold rhodanese efficiently. Thus, although not affecting overall structure, there appear to be irreversible conformational changes induced within the particle. This is similar to what has been reported for GroEL, in that a variety of reagents, including KCl, are able to alter its binding surfaces (Horowitz et al., 1995). Further investigation of the effects of the above reagents may aid in deciphering the mechanism of chaperonin-mediated protein folding.

Materials and methods

Isolation of rabbit reticulocyte TRiC

Reticulocyte lysate (Green Hectares) was quickly thawed by immersing the tubes in water, then made 1 mM in the protease inhibitors PMSF and TAME by adding 100 mM stock solutions in ethanol or water, respectively. While stirring the lysate slowly on ice, solid ammonium sulfate was added to 30% saturation. After 10 min, the suspension was centrifuged at 16,000 × *g* for 20 min at 4 °C. The supernatant was then brought to 50% saturation in ammonium sulfate with stirring and centrifugation as above.

The resulting pellet was suspended in column buffer of 50 mM Hepes, pH 7.2, 5 mM magnesium acetate, 0.5 mM EDTA, 1 mM dithiothreitol, 10% (v/v) glycerol, 1 mM PMSF, 1 mM TAME. The solution was layered over 2-mL cushions of 1 M sucrose in column buffer and centrifuged in 9-mL tubes at 250,000 × *g* for 3 h at 4 °C. The sucrose layer was pipetted from the bottom of the tubes and remaining supernatant discarded. Pellets were resuspended in generous amounts of column buffer, combined with the sucrose layer, and applied to a 2.5 × 10-cm column of heparin-Sepharose™ CL-6B (Pharmacia Biotech) that had been equilibrated with 250 mM KCl in column buffer. After washing with three column volumes of the same buffer, bound material was eluted using a linear gradient to 500 mM KCl over 225 mL. Appropriate fractions were chosen on the basis of SDS-PAGE polypeptide pattern.

The pooled column fractions (50–70 mL) were centrifuged in 32-mL tubes for 5 h at 265,000 × *g* at 4 °C over 5-mL cushions of storage buffer containing 50 mM Hepes, pH 7.4, 1 mM dithiothreitol, 0.5 mM EDTA, 50% (v/v) glycerol. The purified

chaperonin was collected from the bottom 4 mL by piercing the bottom of the tubes and stored at −20 °C.

Analytical methods

SDS-PAGE was according to Laemmli (1970) with Coomassie blue protein staining. Stoichiometry of polypeptides was calculated relative to the 70-kDa band from densities measured on a BioRad model 620 video densitometer.

For amino-terminal sequencing, protein was either blotted from 5% gels onto polyvinylidene difluoride membrane using a semi-dry transfer apparatus (BioRad) with standard blotting buffer (Towbin et al., 1979), or centrifuged onto the membrane using a ProSpin™ cartridge (Applied Biosystems). For blotted protein, bands were visualized with Coomassie blue. In both cases, gas-phase sequencing was performed directly on membrane slices using an Applied Biosystems model 470A protein sequencer. Removal of N-terminal blocking groups was attempted by incubating membrane-bound protein with 0.6 N HCl or anhydrous TFA (LeGendre et al., 1993).

Buffer exchanges were effected using 5-mL HiTrap™ desalting cartridges and protein was further concentrated on 5-mL HiTrap™ heparin cartridges (Pharmacia Biotech). Glycerol density gradients were formed by layering 0.75-mL portions of 20, 25, 30, 35, and 40% (v/v) glycerol in 50 mM Hepes, pH 7.2, 50 mM NaCl in 4-mL tubes. After 4 h of diffusion at room temperature, the gradients were chilled and 0.05–0.1-mL samples (ca. 50 μg of protein) in the same buffer were applied. After centrifugation for 15 h at 150,000 × *g* at 4 °C, ca. 0.2-mL fractions were collected by piercing the bottom of the tubes. Parallel gradients were run with the multienzyme complex of aminoacyl-tRNA synthetases (1.2×10^6 Da, Norcum, 1991), thyroglobulin (670,000 Da), apoferritin (443,000 Da), and catalase (220,000 Da) as mass standards.

Samples for analytical ultracentrifugation were in 20 mM sodium phosphate, pH 7.4. Sedimentation velocity data was collected using standard sector cells in the Beckman-XLA analytical ultracentrifuge. Centrifugation was at 30,000 rpm at 24.6 °C. The apparent *S* value was determined from a Svedberg plot of the logarithm of the change of boundary position as a function of time (Ralston, 1993) and from the time derivative of the concentration profile (Stafford, 1992). Corrections to give $S_{20,w}$ were according to Laue et al. (1992). Calculations assumed a sphere with diameter of 15–18 nm as measured from electron micrographs and a typical protein partial specific volume of 0.725 (Ralston, 1993).

For electron microscopy, samples in storage buffer or fractions from glycerol density gradients were diluted to 10–20 μg/mL in 50 mM Hepes, pH 7.4, 25 mM KCl, adsorbed to thin carbon films, then stained with 1% uranyl acetate using a double carbon technique modified from Lake (1978). Micrographs were taken with a Zeiss EM-10 at an absolute magnification of 80,000.

For freeze/thaw effects, samples were subjected to five cycles of quick freezing in liquid nitrogen and thawing to room temperature. Samples at 0.2 mg/mL were extracted with Triton X-114 as described previously (Norcum, 1991). For salt and nonionic detergent treatment, 0.1 volume of samples at 0.7 mg/mL were added to 17.5 mM DOC, 1.25 M KCl, 1 M LiCl, or 1 M NaSCN. After 15 min at 37 °C, samples were placed on ice and then desalted as above over 5-mL cartridges. For the pH series, samples were diluted to ca. 10 μg/mL with 50 mM ammonium acetate, pH 4.5, 50 mM sodium citrate, pH 6, or 50 mM sodium borate, pH 9, heated 15 min at 37 °C, then placed on ice.

Activity assays

ATPase activity was assayed by measuring orthophosphate release with malachite green color reagent (Lanzetta et al., 1979; Lill et al., 1990). Triplicate samples of four different chaperonin preparations were incubated at 0.1 or 0.25 μM in the presence of 50 mM Hepes, pH 7.2, 10 mM Mg acetate, 5 mM ATP, for 60 min at 37 °C. Values were corrected for sample contamination with phosphate and spontaneous ATP hydrolysis.

Rhodanese (4 mg/mL) and actin (2 mg/mL) were denatured in 6 M guanidine HCl for 2 h at room temperature. Denaturation of rhodanese was verified by the resultant shift of its tryptophan fluorescence emission maximum (Martin et al., 1991). Native proteins at the same concentrations, buffer (25 mM Hepes, pH 7.4, 50 mM KCl), or 6 M guanidine were used for controls. ANS fluorescence was measured with excitation at 325 nm on samples (200 μL) containing 0.25 μM chaperonin and/or substrate proteins with 5 μM 2,6-anilinonaphthalene sulfonic acid. ATP-dependent refolding was conducted for 40 min at 30 °C in aliquots (185 μL) of the same samples after adding 15 μL of 25 mM ATP, 125 mM Mg acetate in the same buffer. Net ANS fluorescence at 430 nm was calculated relative to samples containing no substrate protein, but with the corresponding addition of buffer or guanidine. At this wavelength, the difference between fluorescence with chaperonin alone and with added denatured substrates is maximized. All values are from the average of four spectra.

Acknowledgments

The expertise of Dr. John J. Correia and the University of Mississippi Medical Center Analytical Ultracentrifugation Facility in collection and analysis of the sedimentation velocity data, and Dr. Mark O.J. Olson and Michael Wallace in protein sequencing is gratefully acknowledged. Special thanks are due Dr. V. Gregory Chinchar for numerous discussions and J. Anthony Warrington for protein purifications. Dr. Helen Saibil is thanked for her comments and encouragement. This work was supported in part by USPHS FIRST award GM 40521 and by US Army Research Office grant DAAH04-94-G-0335. Acquisition of the analytical ultracentrifuge was through NSF award BIR 9216150 (J.J.C.).

References

Braig K, Otwinowski Z, Hegde R, Boisvert DC, Joachimiak A, Horwich AL, Sigler PB. 1994. The crystal structure of the bacterial chaperonin GroEL at 2.8 Å. *Nature 371*:578–586.

Braig K, Simon M, Furuya F, Hainfeld JF, Horwich AL. 1993. A polypeptide bound by the chaperonin groEL is localized within a central cavity. *Proc Natl Acad Sci USA 90*:3978–3982.

Chen S, Roseman AM, Hunter AS, Wood SP, Burston SG, Ranson NA, Clarke AR, Saibil HR. 1994. Location of a folding protein and shape changes in GroEL–GroES complexes imaged by cryo-electron microscopy. *Nature 371*:261–264.

Copeland RA. 1994. Detection of non-protein components. In: *Methods for protein analysis: A practical guide to laboratory protocols*. New York: Chapman and Hall. pp 113–125.

Ellis RJ. 1993. The general concept of molecular chaperones. *Phil Trans R Soc Lond B 339*:257–261.

Frydman J, Nimmesgern E, Erdjument-Bromage H, Wall JS, Tempst P, Hartl FU. 1992. Function in protein folding of TRiC, a cytosolic ring complex containing TCP-1 and structurally related subunits. *EMBO J 11*: 4767–4778.

Frydman J, Nimmesgern E, Ohtsuka K, Hartl FU. 1994. Folding of nascent

polypeptide chains in a high molecular mass assembly with molecular chaperones. *Nature 370*:111–117.

Gao Y, Melki R, Walden PD, Lewis SA, Ampe C, Rommelaere H, Vandekerckhove J, Cowan NJ. 1994. A novel cochaperonin that modulates the ATPase activity of cytoplasmic chaperonin. *J Cell Biol 125*:989–996.

Gao Y, Thomas JO, Chow RL, Lee GH, Cowan NJ. 1992. A cytoplasmic chaperonin that catalyzes β-actin folding. *Cell 69*:1043–1050.

Gao Y, Vainberg IE, Chow RL, Cowan NJ. 1993. Two cofactors and cytoplasmic chaperonin are required for the folding of α- and β-tubulin. *Mol Cell Biol 13*:2478–2485.

Gupta RS. 1995. Evolution of the chaperonin families (Hsp60, Hsp10 and Tcp-1) of proteins and the origin of eukaryotic cells. *Mol Microbiol 15*:1–11.

Horowitz PM, Hua S, Gibbons DL. 1995. Hydrophobic surfaces that are hidden in chaperonin cpn60 can be exposed by formation of assembly-competent monomers or by ionic perturbation of the oligomer. *J Biol Chem 270*:1535–1542.

Horwich AL, Willison KR. 1993. Protein folding in the cell: Functions of two families of molecular chaperone, hsp 60 and TF55-TCP1. *Phil Trans R Soc Lond B 339*:313–326.

Hynes G, Kubota H, Willison KR. 1995. Antibody characterisation of two distinct conformations of the chaperonin-containing TCP-1 from mouse testis. *FEBS Lett 358*:129–132.

Kellenberger E, Häner M, Wurtz M. 1982. The wrapping phenomenon in air-dried negatively stained preparations. *Ultramicroscopy 9*:139–150.

Kubota H, Hynes G, Carne A, Ashworth A, Willison K. 1994. Identification of six *Tcp-1*-related genes encoding divergent subunits of the TCP-1-containing chaperonin. *Curr Biol 4*:89–99.

Kubota H, Hynes G, Willison K. 1995. The chaperonin containing *t*-complex polypeptide (TCP-1), multisubunit machinery assisting protein folding and assembly in the eukaryotic cytosol. *Eur J Biochem 230*:3–16.

Laemmli UK. 1970. Cleavage of structural proteins during the assembly of the head of bacteriophage T4. *Nature 227*:680–685.

Lake JA. 1978. Electron microscopy of specific proteins: Three-dimensional mapping of ribosomal proteins using antibody labels. In: Koehler JK, ed. *Advanced techniques in biological electron microscopy, volume 2*. New York: Springer-Verlag. pp 173–211.

Langer T, Pfeifer G, Martin J, Baumeister W, Hartl FU. 1992. Chaperonin-mediated protein folding: GroES binds to one end of the groEL cylinder, which accommodates the protein substrate within its central cavity. *EMBO J 11*:4757–4765.

Lanzetta PA, Alvarez LJ, Reinach PS, Candia OA. 1979. An improved assay for nanomole amounts of inorganic phosphate. *Anal Biochem 100*:95–97.

Laue TM, Shah BD, Ridgeway TM, Pelletier SL. 1992. Computer-aided interpretation of analytical sedimentation data for proteins. In: Harding SE, Rowe AJ, Horton JC, eds. *Analytical ultracentrifugation in biochemistry and polymer science*. Cambridge: Royal Society of Chemistry. pp 90–125.

LeGendre N, Mansfield M, Weiss A, Matsudaira P. 1993. Purification of proteins and peptides by SDS-PAGE. In: Matsudaira P, ed. *A practical guide to protein and peptide purification for microsequencing, 2nd ed.* San Diego: Academic Press. pp 71–101.

Lewis VA, Hynes GM, Zheng D, Saibil H, Willison K. 1992. T-complex polypeptide-1 is a subunit of a heteromeric particle in the eukaryotic cytosol. *Nature 358*:249–252.

Lill R, Dowhan W, Wickner W. 1990. The ATPase activity of secA is regulated by acidic phospholipids, secY, and the leader and mature domains of precursor proteins. *Cell 60*:271–280.

Lingappa JR, Martin RL, Wong ML, Ganem D, Welch WJ, Lingappa VR. 1994. A eukaryotic cytosolic chaperonin is associated with a high molecular weight intermediate in the assembly of hepatitis B virus capsid, a multimeric particle. *J Cell Biol 125*:99–111.

Marco S, Carrascosa JL, Valpuesta JM. 1994. Reversible interaction of β-actin along the channel of the TCP-1 cytoplasmic chaperonin. *Biophys J 67*:364–368.

Martin J, Langer T, Boteva R, Schramel A, Horwich AL, Hartl FU. 1991. Chaperonin-mediated protein folding at the surface of groEL through a "molten globule"-like intermediate. *Nature 352*:36–42.

Melki R, Cowan NJ. 1994. Facilitated folding of actins and tubulin occurs via a nucleotide-dependent interaction between cytoplasmic chaperonin and distinctive folding intermediates. *Mol Cell Biol 14*:2895–2904.

Mock DM, Lankford G, Horowitz P. 1988. A study of the interaction of avidin with 2-anilinonaphthalene-6-sulfonic acid as a probe of the biotin binding site. *Biochim Biophys Acta 956*:23–29.

Norcum MT. 1991. Structural analysis of the high molecular mass aminoacyl-tRNA synthetase complex—Effect of neutral salts and detergents. *J Biol Chem 266*:15398–15405.

Oliver RM. 1973. Negative stain electron microscopy of protein macromolecules. *Methods Enzymol 27*:616–672.

Phipps BM, Typke D, Hegerl R, Volker S, Hoffman A, Stetter KO, Baumeister W. 1993. Structure of a molecular chaperone from a thermophilic archaebacterium. *Nature 361*:475–477.

Ralston G. 1993. *Introduction to analytical ultracentrifugation*. Fullerton, California: Beckman Instruments, Inc.

Rommelaere H, Van Troys M, Gao Y, Melki R, Cowan NJ, Vandekerckhove J, Ampe C. 1993. Eukaryotic cytosolic chaperonin contains t-complex polypeptide 1 and seven related subunits. *Proc Natl Acad Sci USA 90*:11975–11979.

Roobol A, Holmes FE, Hayes NV, Raines AJ, Carden MJ. 1995. Cytoplasmic chaperonin complexes enter neurites developing in vitro and differ in subunit composition within single cells. *J Cell Sci 108*:1477–1488.

Saibil H, Wood S. 1993. Chaperonins. *Curr Opin Struct Biol 3*:207–213.

Stafford WF. 1992. Boundary analysis in sedimentation transport experiments: A procedure for obtaining sedimentation coefficient distributions using the time derivative of the concentration profile. *Anal Biochem 203*:295–301.

Thornton DJ, Carlstedt I, Sheehan JK. 1994. Identification of glycoproteins on nitrocellulose membranes and gels. In: Walker JM, ed. *Methods in molecular biology, vol 32: Basic protein and peptide protocols*. Totowa, New Jersey: Humana Press. pp 119–128.

Todd MJ, Lorimer GH. 1995. Stability of the asymmetric *Escherichia coli* chaperonin complex—Guanidine chloride causes rapid dissociation. *J Biol Chem 270*:5388–5394.

Towbin H, Staehlin T, Gordon J. 1979. Electrophoretic transfer of proteins from polyacrylamide gels to nitrocellulose sheets: Procedure and some applications. *Proc Natl Acad Sci USA 76*:4350–4354.

Waldmann T, Nimmesgern E, Nitsch M, Peters J, Pfeifer G, Müller S, Kellermann J, Engel A, Hartl FU, Baumeister W. 1995. The thermosome of *Thermoplasma acidophilum* and its relationship to the eukaryotic chaperonin TRiC. *Eur J Biochem 227*:848–856.

Yaffe MB, Farr GW, Miklos D, Horwich AL, Sternlicht ML, Sternlicht H. 1992. TCP1 complex is a molecular chaperone in tubulin biogenesis. *Nature 358*:245–248.